SPACEMAP: The Prediction and Avoidance of Radio Frequency Interference using Dynamic Voronoi Diagram

Peter Joonghyun Ryu*
SPACEMAP Inc.
Shawn Seunghwan Choi*
SPACEMAP Inc.
Jaedong Seong*
Korea Aerospace Research Institute
Misoon Mah
M&K Research & Development
Douglas Deok-Soo Kim
SPACEMAP Inc.

*These authors equally contributed to this paper.

Geo-space is already busy by space objects and will be busier. More satellites are being deployed and spectrum space is also becoming more congested by their radio frequency (RF) for communications to/from both ground stations and other satellites. One of the critical consequences of the congested spectrum space and busy geo-space is radio frequency interference (RFI) which may cause serious communication disruption. For example, satellite operators occasionally experience failure to download images due to RFI. This phenomenon will be outstanding as more constellations will be in orbits, e.g., Stralink, Oneweb, Planet, etc. Therefore, the prediction of RFI, and hopefully followed by its mitigation, is crucial for smooth communication. However, the prediction and mitigation are computational challenges for the satellites orbiting at extreme speeds, particularly in the forthcoming constellations of from hundreds to thousands, if not tens of thousands, of satellites. This is because an RFI occurs under specific geometric conditions involving (i) three or (ii) four objects at least, depending on conditions. The first obvious case consists of two orbiting satellites, own-sat O and adversarial-sat A, and a ground station G. In this case, A enters the communication field-of-view (FoV) of O with respect to G. So, it is necessary to explore the combinatorial space of (N, 3) where N represents the number of satellites plus ground stations, for each moment in timeline. The second case consists of two orbiting satellites, O and A, and two ground stations, G(O) and G(A) for O and A, respectively. In this case, O enters the FoV of A with respect to G(A) while it maintains communication with G(O). So, the size of the combinatorial space is of (N, 4) for each moment in timeline. The cases of higher combinatorial space may not be ignorable. Here we introduce the SPACEMAP feature which can efficiently and accurately predict the RFI of own satellites against all known radio-frequency emitting objects in space catalogue. We aim to present the best-possible solutions in near real-time. This challenging objective is being materialized by the Voronoi diagram which is the most compact and concise data structure of particles in 3D space, in particular, the dynamic Voronoi diagram of fast-moving space objects to define the extreme spatiotemporal proximity. Assuming a preprocessing operation to construct the Voronoi diagram over timeline, the SPACEMAP method can solve many challenging spatiotemporal problems very fast, i.e., near real-time if not truly real-time. This study makes the following additional contributions. First, the method used for the RFI prediction can be similarly used to find a way for RFI avoidance. Second, the RFI prediction provides a mitigate scheme to avoid corrupted communication due to noise. Third, the SPACEMAP function can be used for retrospective analysis for either known or unknown past RFIs of own satellites. It is also important to note that the Voronoi diagram database by the preprocessing can be used to solve a variety of problems because it is application neutral.

1. INTRODUCTION

Thousands of satellites are functional from those deployed ever since Sputnik in 1957. It seems that more than 100,000 new satellites to be deployed in the forthcoming decade. Two primary mission types are sensing and communications: Remote sensing for making observations and measurements of the Earth or space and communications for to and from ground stations or between satellites. Recent developments for space-based space-situational awareness (SSA) add another important avenue to measurement. The two mission types in principle produce-&-transmit data and therefore eventually need to up- and down-link between satellites and ground stations. Other types of satellites such as those for security and defense usually have the same functionality, too. The emerging blue ocean called ISAM (In-orbit servicing, assembly, and manufacturing) must contain these functions as well.

There are in principle two media used for satellite communications: radio frequency (RF) and optics. RF has long played the primary role in space communications. While it is easy, convenient, and cheap, it has drawbacks. RF is vulnerable to hacking and jamming as an RF interference (RFI) can be easily designed and implemented. E.g., see the AFRL's Hack-A-Sat hacking competition [1]. In addition, RF itself is a limited human resource to be shared by all and an ITU permission is required for new satellites. Optical communications such as using laser, on the other hand, is becoming popular due to its several advantageous features. Its data bandwidth is much higher than RF. It is more robust for hacking, jamming, interference, etc. than RF. In addition, the intervention by ITU is less expected. Laser communications between satellites and ground stations and between satellites via inter-satellite link (ISL) are becoming blue ocean. To maximize the utilization of communication constellations, it is beneficial to have the neighborhood information among satellites in timeline beforehand.

Despite the advantages of optical communications, RF will remain one of the principal media due to its aforementioned merits. Particularly in the heterogeneous space environment where multi-constellations operating in multi-orbits by multi-operators, the RFI-related issues are and will be critical to the safety and sustainability of space business. Therefore, it is necessary to design interference-free satellites operating environment using RF communications. However, there does not exist a good computational method both for the design of RFI-free or RFI-less-vulnerable satellites communication systems and for the prediction of RFI and the avoidance strategies of predicted interferences. Here we introduce a computational method to predict potential RFI events between satellites and ground stations in timeline. Then, a strategy for the deconfliction of predicted interference events can be easily facilitated. The presented method can be immediately applied to more challenging problems such as developing a methodology for the maximal use of the radio frequency resource for space communication. The method aims at presenting real-time response to both problems using a unified method based on computational geometry construct called the Voronoi diagram [3, 4], in particular its dynamic version for moving satellites in the 3D space [5]. The target input data size for real-time response for the prediction of RFI is the soon-expected $O(10^5) \sim O(10^6)$ communication satellites within a decade. Our current code already shows sufficiently fast speed, if not real-time yet, for currently anticipated users such as Starlink, OneWeb, and Kuiper.

We note that satellites are moving in the geospace which also contains many other types of objects such as debris, rocket bodies, etc. Recent study reports O(10K) objects of size >10cm, O(1M) ones of size 1cm ~ 10cm, and O(100M) ones of size 0.1cm ~ 1cm [6]. We want to emphasize that the SpaceMap method solves both the RFI-related problems and the conjunction assessment and collision avoidance in near real-time in a unified computational framework.

Section 2 defines the RFI problem. Section 3 presents the computational size of the RFI problem using filtration concept and Voronoi diagram. Section 4 presents the experimental results which shows important properties of the RFI problem. Section 5 presents the algorithm to solve the RFI problem using the Voronoi diagram. Section 6 concludes this study.

2. MODELING RADIO FREQUENCY INTERFERENCE

Here we present a mathematical model for data transmission with sources and receivers. For convenience of presentation, we consider only downlink transmission: RF is coming from space to ground. Hence, ground station is a receiver R and satellite is a source S. Similar observation holds for uplink and inter-satellite link as well. RFI, also called electromagnetic interference, is a disturbance phenomenon in the RF spectrum due to electromagnetic induction, electrostatic coupling, or conduction [7]. It increases error rate and can be used for intentional radio jamming in electronic warfare. ITU defines it as follows [8]: "The effect of unwanted energy due to one or a combination of emissions, radiations, or inductions upon reception in a radiocommunication system, manifested by any performance degradation, misinterpretation, or loss of information which could be extracted in the absence of such unwanted energy". Fig. 1 shows an example of the interference experienced by GK-2A satellite in GEO [9]. The horizontal and vertical axes are frequency and SNR, respectively. The peak in the red box is the noise due to the interference caused by KOMPSAT-2 satellite in LEO. Interestingly enough, the two satellites in this example are both owned and operated by Korea Aerospace Research Institute (KARI) in Daejeon, Korea.

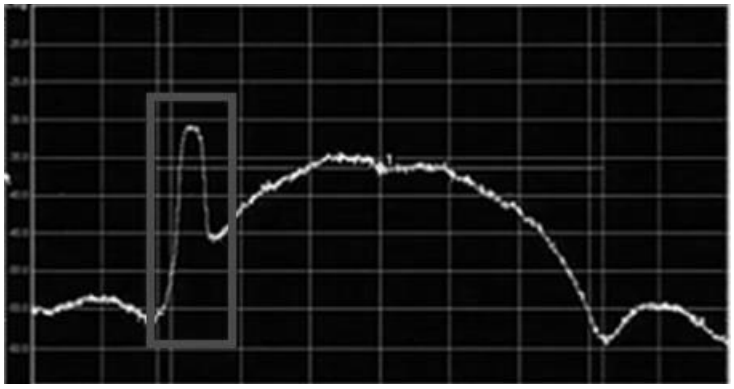

Fig. 1. An RFI example. Horizontal axis: Frequency. Vertical axis: SNR. Source satellite (Satellite-of-interest): GK-2A in GEO. Secondary satellite: KOMPSAT-2 in LEO. Quoted from [9]

We model RFI as a function

$$RFI = f(G, F, P) \tag{1}$$

of three major variables where G, F, and P denote geometry, frequency, and power density, respectively. Observe that $G = G(t)$ is a function of time t while F and P are constants. When receiver R and two sources S1 and S2 are colinear within an angular tolerance τ in the same linear half-space of R, the two RFs of S1 and S2 may interfere if two additional conditions for frequencies and power densities are satisfied. Here let S1 be the **primary**, i.e., the own satellite-of-interest, and S2 the **secondary**. Hence, we view the geometric collinearity as the necessary condition for interference meaning that the geometric filter **G-filter** is a precondition for additionally applying **F-** and **P-filters**. If the angle $\angle(S1, R, S2)$ is greater than τ, S2 is called **non-disturbing** for S1. We first apply the G-filter for R and S1 to reduce solution space as small and quick as possible by removing non-disturbing satellites for each moment in timeline. We call it the **filtration** that applying the G-filter to filter out non-disturbing satellites for each pair of source and receiver in timeline. Let Dsset(S1) be the set of TLE satellites which disturb S1's data transmission over the prediction window W. Let PrimarySet and SecondarySet be the sets of primary and secondary satellites, respectively. Then, a filtration is defined as

$$Dsset(S1) \leftarrow Filtration(S1, SecondarySet, \tau, W). \tag{2}$$

The size of Dsset is usually small. The size of PrimarySet is also usually small: e.g., $O(1) \sim O(10)$ for most satellite owners, $O(10^2)$ for a few such as OneWeb, Planet, and Spire, but is already $O(10^3)$ and will be soon $O(10^4)$ for Starlink. The size of the SecondarySet in the TLE database is currently $O(10^3)$ and will be soon $O(10^4)$.
We further define a **FILTRATION** as a filtration from the Cartesian product of PrimarySet and SecondarySet as follows.

$$DSSET(PrimarySet) \leftarrow FILTRATION(PrimarySet, SecondarySet, \tau, W). \tag{3}$$

Here DSSET is the set of disturbing satellites corresponding to the Cartesian product. Hence, the quick and accurate filtration of non-disturbing payloads for a timeline with length 1 ~ 24 hours is challenging, e.g., if 1 Hz sampling rate is employed, particularly when there are multiple ground stations, say M. Let TimeFilter and TimeFILTER be the computation time for Eq.s (2) and (3), respectively. Unless a clever algorithm is used, TimeFILTER = M*|PrimarySet|*TimeFilter for M ground stations. In this study, we assume the angular tolerance τ of the G-filter as 1 degree. Note that the ordinary LEO orbit period of 90min corresponds to 0.067 degrees/sec. We note that the RFI function in Eq. (1) is neither necessarily linear to G, F, and P nor G, F, and P are independent of each other. However, in this initial report, we assume that they are independent of each other. Fig. 2 illustrates a schematic diagram of geometric interference condition and a walk-around of the predicted interference via a friendly neighborhood. When an interference is predicted, there may be other avoidance strategies as well: E.g. not transmitting data while the interference condition is maintained, transmitting data to another ground station in the proximity of the given ground station if possible, etc.

Filtration leaves relatively few disturbing satellites in timeline. Therefore, testing (i) if two satellites' frequency overlap and (ii) the secondary's power density is strong enough to cause an interference to the primary can be done O(1) time for each payload. Hence, applying F- and P-filters takes does not take long if it is not O(1) time when the filtration leaves a small set, which is mostly the case. Other rare cases yet with a higher complication will not be discussed here. E.g., two ground stations and two satellites, i.e., R1, R2, S1, and S2.

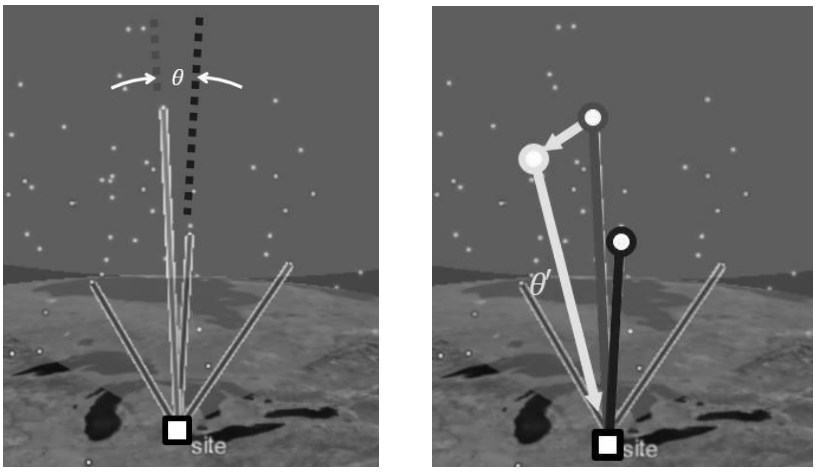

Fig. 2. Geometric filter for RFI prediction and its avoidance by walk-around. (a) If $\theta < \tau$, an RFI may exist. θ is an angular distance between the red and blue. (b) Once an interference is predicted, deconfliction alternatives can be devised. In this schematic diagram, a friendly neighbor satellite of the red one can be identified so that data can be transmitted seamlessly via the walk-around route through the yellow one. Another strategy might be to stop transmitting data while the geometric condition for interference holds. A third might be to transmit data to neighbor sites. All avoidance strategies can be identified in O(1) time as there are only O(1) friendly objects around.

3. FILTRATION VIA GEOMETRIC FILITER USING VORONOI DIAGRAM

Filtration is to apply G-filter at each moment in timeline. Applying G-filter at a moment consists of two steps: (i) Finding candidate satellites for R and (ii) applying the geometric filter for R and S1. In this section, we assume that the antenna of ground station has a fixed orientation, FoV, and range.

The first step is a direct application of WatcherCatcher functionality of SpaceMap [10]. Given the coordinate of a site on the Earth surface (i.e., latitude, longitude, and altitude), the field-of-view (FoV) of a visibility cone, and the distance limit of sensor, WatcherCatcher efficiently finds the space objects within the cone at the site in timeline. The second step is to apply the G-filter to the output of the first step. Suppose that we found a set CandSSet={CS1, CS2, .., CSm} of source satellites within the visibility cone at an arbitrary moment. As the calculation of $\angle$(S1, R,

CSi) takes O(1) time, scanning CandSSet for the angle calculation takes O(m) time. Fig. 3 shows the WatcherCatcher output at KARI as the yellow visibility cone with the FoV of 120 degrees at an arbitrary moment. The line segments correspond to the satellites captured by the cone. The blue line segment denotes the primary satellite has entered the cone so that the communication channel is connected to the ground station. The red line segments denote the satellites which define the angular distance less than τ. The black line segments correspond to the other satellites within the cone.

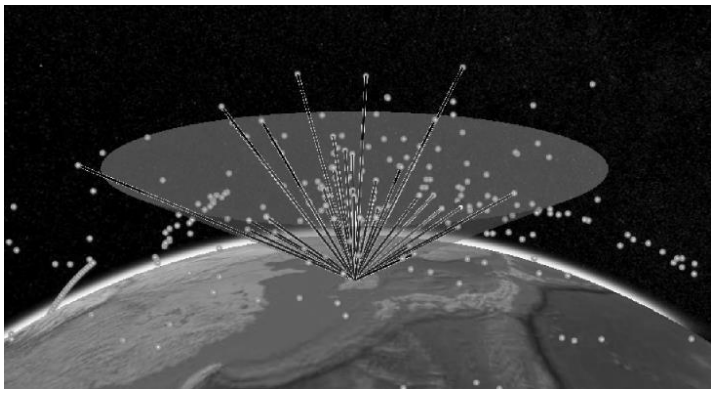

Fig. 3. WatcherCatcher output at Daejeon, Korea. Visibility cone FoV: 120 degrees. Range: 2,000 km. Line segments correspond to the satellites in the cone. Blue line segment: the primary satellite. Red: the satellites with the angular distance less than τ. Black: other satellites within the cone.

The underpinning computational theory of the WatcherCatcher is the Voronoi diagram of 3D particles which represent satellites. Voronoi diagram is the tessellation of space using input generators where an arbitrary location in a cell is closer to its owner generator than to any other generator. While the distance can be defined differently, the ordinary Euclidean distance is most common. It has been well-known that the Voronoi diagrams are the most concise data structure to capture the proximity of generators and spatial queries can be most efficiently answered if its topological structure is properly represented and used. Fig. 4 shows the Voronoi diagram of 2D points. We store the topological structure in the Winged-Edge data structure which takes O(M) memory for M generators. Then, neighborhood search can be done very efficiently. The red dotted line segment in the figure denotes the neighbor generators of the one, say G, in the center which share cell boundary with G. If there are m such neighbors, all of them can be found in O(m) time from G using the Winged-Edge data structure. In 2D, $m = 6$ on average while it may vary depending on the distribution of generator locations. Note that m is independent of M.

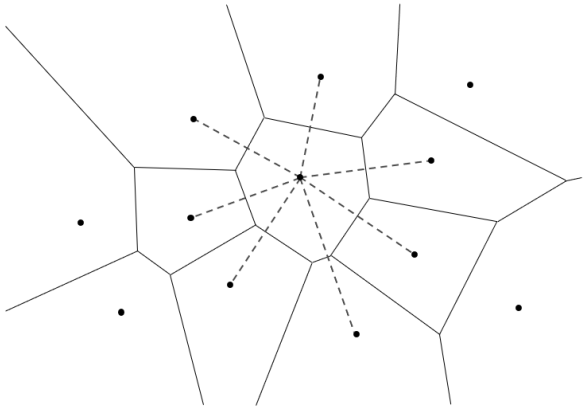

Fig. 4. Voronoi diagram of twelve point generators in 2D. The Euclidean distance is used. The red line segment denotes the neighborhood of the point generator in the center, say G. If this Voronoi diagram is stored in the Winged-Edge data structure, the m neighbors of G can be found from G in O(m) time.

If the arrangement of point generators is stored in the Voronoi diagram structure, useful queries can be answered fast. Suppose that we want to find the neighbors of the red line segment connecting the green and blue points. Suppose that we want to find the "neighbors" whose cells intersect with the red line segment. Starting from the green generator, we find its neighbors and test their cells to find an intersecting one, say X, on its cell boundary shared by the green with the line segment. If X is found, we repeat the same procedure. Iterating this procedure eventually reaches the blue generator. When there are m red generators, m=6 in this example, O(m) time is sufficient to find all red generators. Suppose that we want to find the first-order neighbors of the green, blue, and red generators: I.e., we want to find the yellow ones. Then, we propagate the neighborhood search as before from these generators. If there are m yellow ones, O(m) time is sufficient to find all yellow ones: m=17 in this example. Advanced queries involving more complicated spatial conditions can mostly be solved very efficiently using this neighborhood propagation properties of Voronoi diagrams. An example of advanced queries is to find the generators between the red and blue line segments in the figure. These generators can also be found by repeating the propagation a few more times until the blue line segment is reached. Similarly, the solution contains m generators, O(m) time is sufficient to find the solution. Note that all solutions are found with the computation effort independently of the input size. The effort linear to the number of generators in the solution is sufficient! This observation identically holds for 3D cases, too, of course with additional algorithmic complications which we skip to mention here. Emphasis: This complexity is in the worst-case scenario, not on average. Recall that we want to repeat this computation at 1 Hz rate for multiple ground stations. Hence, the computational efficiency of the first step of G-filter is critical.

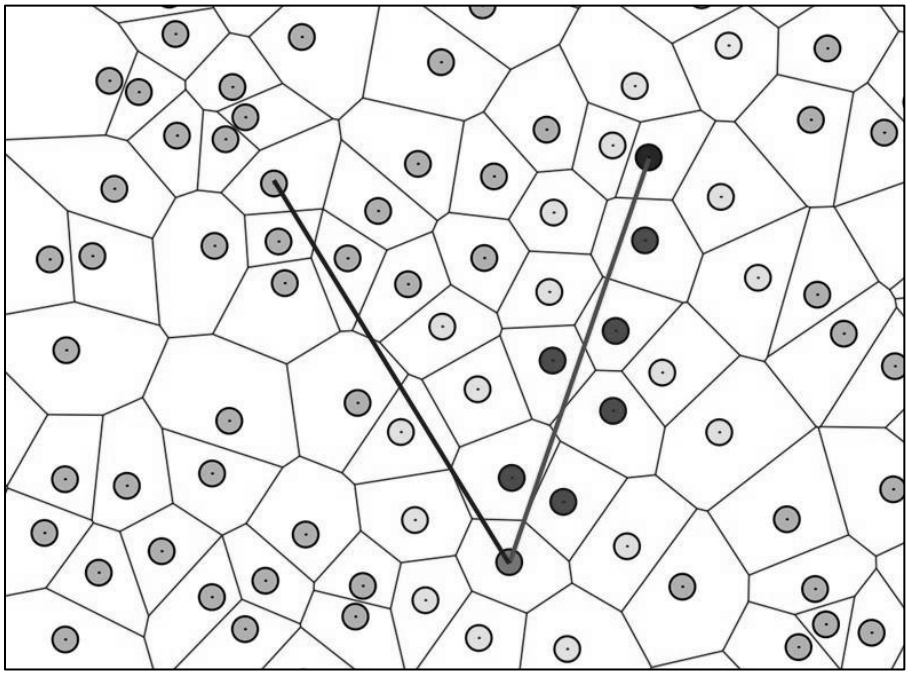

Fig. 5. Neighborhood search using the topology structure of the Voronoi diagram. The m (=6) red generators can be found in O(m) time starting from the green toward the blue. The m (=17) yellow generators can be similarly found in O(m) time. The generators between the red and blue line segments can be found in the linear time to the number of generators in the solution.

4. EXPERIMENTS TO SHOW THE PROPERTIES OF THE RFI PROBLEM

We applied the filtration using three ground stations and four satellites-of-interest. Fig. 6 shows a view that all the seven entities are visible. The experiment was done using the resources owned and operated by KARI. We selected three antennas ((i) Jeju island, South Korea (yellow), (ii) Svalbard, Norway (blue), (iii) Neustrelitz, Germany (green-yellow)). All FoV's are assumed as 120 degrees. The PrimarySet consists of four satellites-of-interest (red dots) owned and operated by KARI: {Sat {CAS500-1 (Norad ID: 47932), KOMPSAT-3 (38338), KOMPSAT-3A (40536), KOMPSAT-5 (39227))}. The TLE data was downloaded @ 2023-08-27T00:00:00Z.

The experiments were conducted on a desktop computer: an AMD RYZEN Threadripper 3995wx @ 2.7GHz, 64Cores with 512GB RAM. All computation was done using SpaceMap's in-house developed AstroLibrary. The TLE data is downloaded at 2023-08-27. Prediction window is 1 hour.

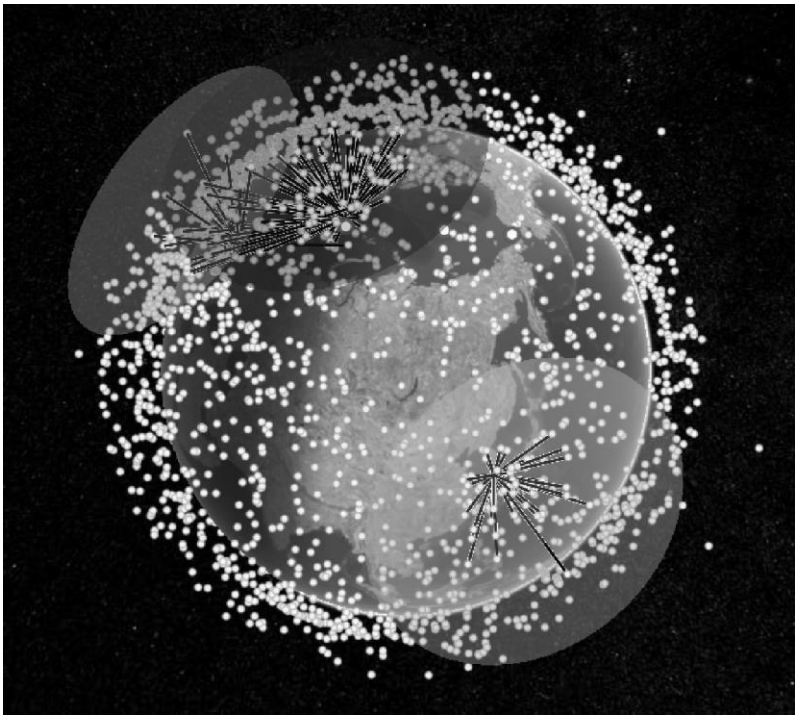

Fig. 6. The visibility cones of the three antenna sites of KARI: (i) Jeju Island, South Korea (yellow), (ii) Svalbard, Norway (blue), (iii) Neustrelitz, Germany (green-yellow). The PrimarySet consists of four satellites-of-interest (red dots) owned and operated by KARI: {CAS500-1 (Norad ID: 47932), KOMPSAT-3 (38338), KOMPSAT-3A (40536), KOMPSAT-5 (39227))}. Green dots denote the satellites captured by the three visibility cones during the prediction window. FoV: 120 deg, TLE downloaded @ 2023-08-27T00:00:00Z.

Fig. 7 shows the statistics of FILTRATION w.r.t. angle threshold (1 ~ 10 degrees) and FoV (80 ~ 160 degrees): the cardinality of DSSET(PrimarySet) and computation time. Computation time super-linearly increases for both variables. Note the order-of-magnitude difference between the two types of angles. The cardinality of DSSET is very sensitive to angle threshold. Fig. 8 shows the enlargement of Fig. 7(a) and (b) in the angle threshold 1 ~ 3 degrees where RFI is likely to occur. Fig. 9 shows the statistics of FILTRATION w.r.t. #Satellites-of-interest and #ground stations.

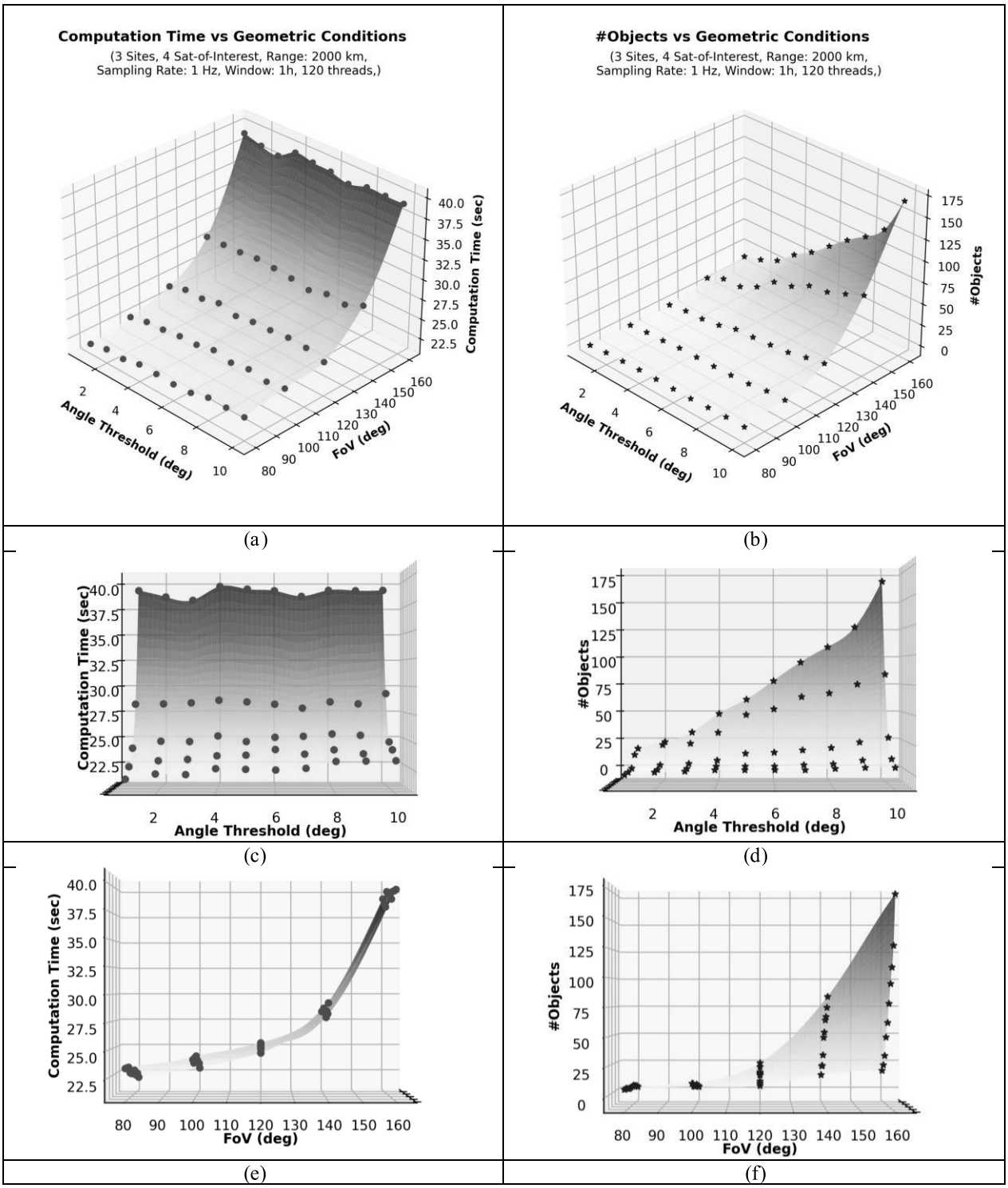

Fig. 7. Statistics of FILTRATION, i.e., applying the G-filter to all three ground stations for all four satellites-of-interest. Left column: Computation time. Right column: #Disturbing satellites. Window length: 1 hour. Range: 2,000 km, Sampling rate: 1 Hz. (a, b) Bird's eye view. Angle threshold τ varies 1 ~ 10 degrees. FoV varies 80 ~ 160 degrees. (c, d) Horizontal axis: Angle threshold. (e, f) Horizontal axis: FoV.

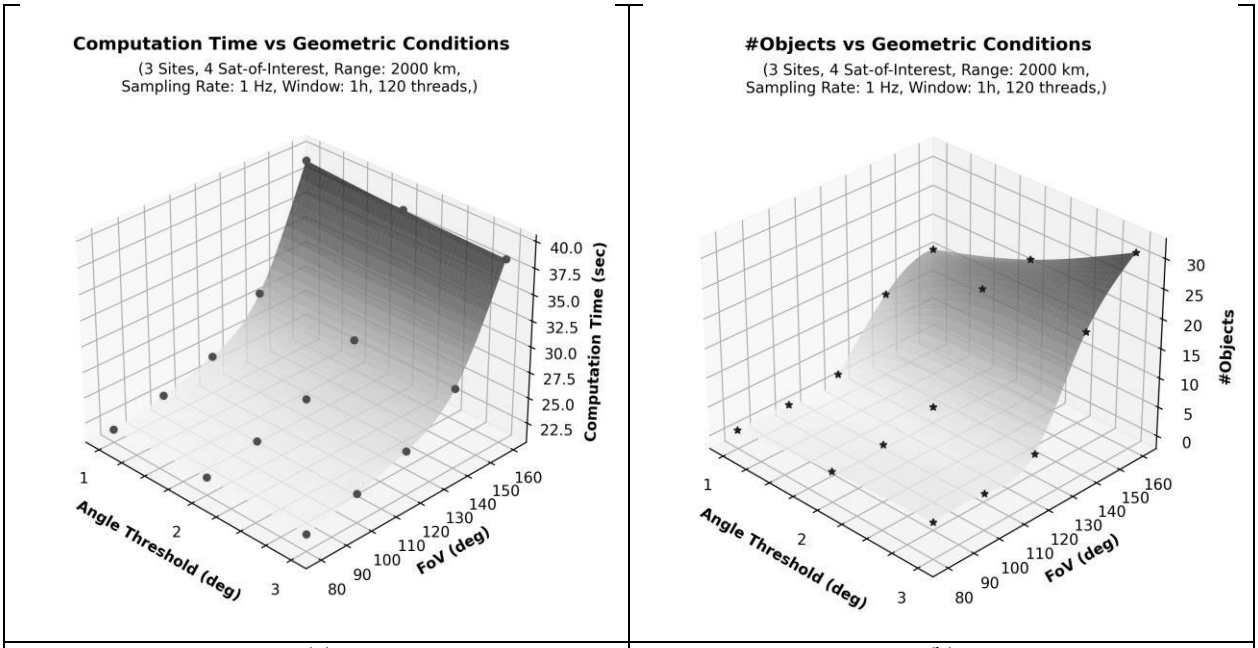

(a) (b)

Fig. 8. Zoom-in of Fig. 7 in the angle threshold 1~3 degrees. Window length: 1 hour. Range: 2,000 km, Sampling rate: 1 Hz. (a) Computation time. (b) #Objects.

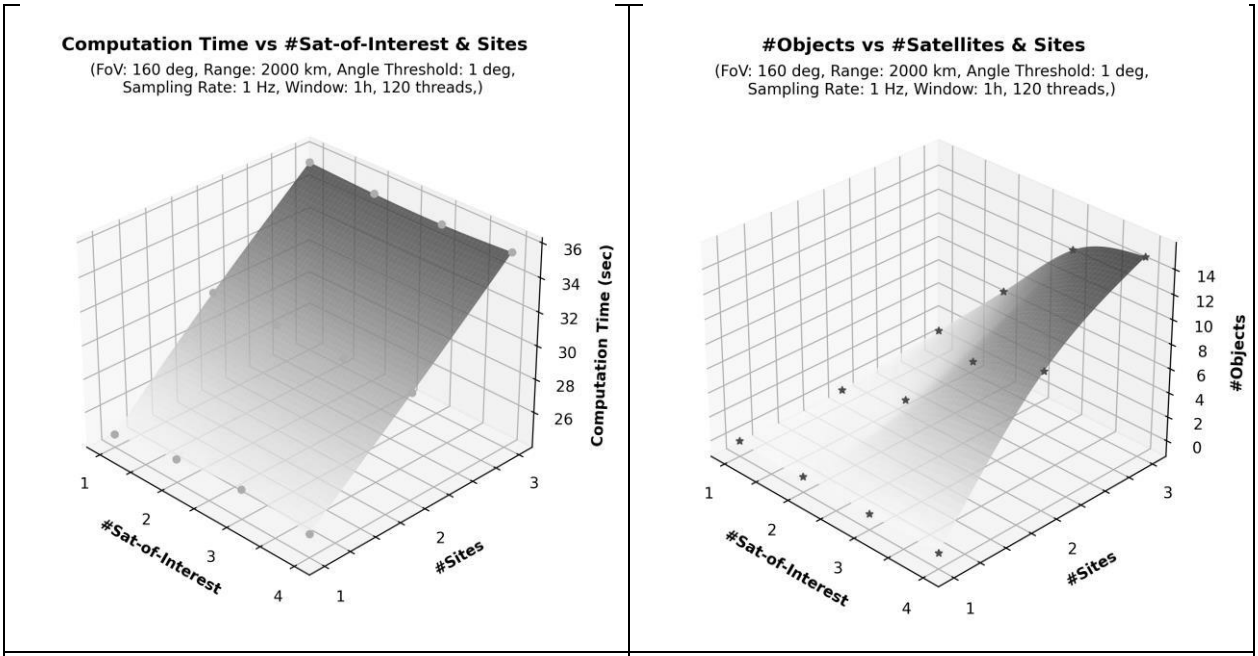

(a) (b)

Fig 9. Statistics of FILTRATION for #Satellites-of-interest and #ground stations. Left column: Computation time. Right column: #Disturbing satellites. Window length: 1 hour. Range: 2,000 km, Sampling rate: 1 Hz. (a, b) Bird's eye view. #Satellites-of-interest varies 1 ~ 4. #Ground stations varies 1 ~ 3. (c, d) Horizontal axis: #Satellites-of-interest. (e, f) Horizontal axis: #Sites.

5. ASTRORFI ALGORITHM FOR THE RFI PROBLEMS

The experimental results above well-describes the properties of the RFI problem such as problem size, etc. which has an immediate influence on a brute force algorithm to solve the problem. Computational efficiency, however, can be significantly improved if the advantageous features of Voronoi diagrams are properly exploited.

Consider a satellite Sat-i. From time to time, Sat-i may be captured by the visibility cone of one of the ground stations. Let a **captive interval set**

$$\text{CaptIntervalSet}(i) = \{[t^i(1,s), t^i(1,e)], [t^i(2,s), t^i(2,e)], .., [t^i(m,s), t^i(m,e)]\} \quad (4)$$

be such an interval set where each element corresponds to the state that Sat-i is captured by the visibility cone of one of the ground stations. Given the captive interval sets of all satellites-of-interest, we make the union of all the captive interval sets. Then, we merge the intervals with common intersections to produce the following interval set

$$\text{CAPTINTERVALSET} = \{[t(1,s), t(1,e)], [t(2,s), t(2,e)], .., [t(n,s), t(n,e)]\} = \{I\_1, I\_2, .., I\_n\} \quad (5)$$

where each interval denotes that at least one of the satellites is captured by one of the ground stations. Hence, we only need to do RFI predictions for the time intervals in CAPTINTERVALSET.

The computation of each moment of the events in Eq.s (4) and (5) requires solving the intersection between a rotating cone with FoV (=120 degrees in the example in this study) and moving space object. Suppose that this problem is solved by an algorithm Algorithm_SatCrossesCone.

Consider an element I = [t_s, t_e] of the interval set where a satellite-of-interest Sat is captured by a ground station Site. Let an interference cone IntfCone be the circular cone with (i) its apex at Site, (ii) its centerline passes through Sat, and (iii) its field-of-view (fov) of τ (=1 degree). The interference cone accompanies Sat while it propagates in I together with all other secondary satellites in the entire TLE data base. During the propagation, we apply Algorithm_ SatCrossesCone using the interference cone and each secondary satellite in the neighborhood of Sat. Then, all time intervals for RFI are computed in INTFRINTERVALSET which is a set of time intervals corresponding to RFI intervals.

We devise two versions of algorithm for solving the RFI problems depending on the size of constellation based on the experimental results above. First, consider a relatively small constellation consisting of O(1) ~ O(10) satellites-of-interest in PrimarySet. In this case, the portion of the intervals in CAPTINTERVALSET in the prediction window is relatively small. We construct two dynamic Voronoi diagrams during the pre-processing. Let SiteSet and PrimarySet be the sets of ground stations and satellites-of-interest, respectively. Let SET-SP be the union of SiteSet and PrimarySet. We construct the dynamic Voronoi diagram DVD-SP of SET-SP and the dynamic Voronoi diagram DVD-TLE of the entire TLE data over a prediction window. Then, we use DVD-SP to quickly compute CAPTINTERVALSET. The size of SET-SP is small and the computation time for DVD-SP is marginal. Then, we use DVD-TLE to compute INTFRINTERVALSET. This approach of separating two DVDs speeds up the computation significantly compared to the experiment given above.
Secondly, consider mega-constellations such as Starlink or OneWeb. In this case, we construct only one dynamic Voronoi diagram for both primary and secondary satellites. This is because one of the satellites must be captured by one of the visibility cones of the ground stations. In order to find the boundary between the two approaches, we need to do further analysis.

6. CONCLUSIONS

Satellites make observations and transmit observed data to ground stations or to other satellites. If two satellites using same radio frequency are collinear with a ground station, their data transmission can be in danger of radio frequency interference (RFI). As there are many satellites and there will be many more in forthcoming years, the RFI problem will be increasingly critical for the safety, efficiency, and sustainability of space activities. The current satellite count $O(10^3)$ will soon reach to $O(10^4)$ and to $O(10^5)$. Therefore, the prediction of RFI of own satellites or satellites-of-interest and deconfliction of predicted interference are critical. However, computationally efficient prediction methods are not sufficiently studied yet.

Here we defined the RFI problem, analyzed its computational challenges, and presented an algorithm for its prediction and deconfliction of predicted interference using dynamic Voronoi diagram of moving satellites in geo-orbit. Given the modeling of an RFI problem as a function of satellites' geometry, frequency, and power, we presented an efficient combinatorial search space reduction method by deriving a necessary condition for interference based on geometry. The frequency and power conditions can be later applied to the reduced search space.

The developed algorithm can be used both as a function in the SpaceMap platform and as an API of AstroLibrary available from SpaceMap.

7. References

[1] HACK-A-SAT 3, AFRL, 2022, (https://afresearchlab.com/lablife/hack-a-sat-3/)
[2] C. Song, J. Cha, M. Lee, and D. S. Kim. Dynamic Voronoi Diagram for Moving Disks, *IEEE Transactions on Visualization and Computer Graphics*, 2021.
[4] A. Okabe, B. Boots, K. Sugihara, and S. N. Chiu. *Spatial Tessellations: Concepts and Applications of Voronoi Diagrams (2nd ed.)*, John Wiley & Sons, Chichester, 1999.
[5] F. P. Preparata, M. I. Shamos. *Computational Geometry: An Introduction (Texts and Monographs in Computer Science) (1st ed.),* Springer, 1985.
[6] ESA Space Debris Office, ESA'S ANNUAL SPACE ENVIRONMENT REPORT(7.0) , GEN-DB-LOG-00288-OPS-SD, 12 June, 2023
[7] Electromagnetic interference, *WIKIPEDIA*, 2023 (https://en.wikipedia.org/wiki/Electromagnetic_interference)
[8] The International Telecommunication Union's (ITU), *Radio Regulations (RR)*, 2020 edition, Vol 1.
[9] J. Seong, O. Jung, Y. Jung, S. Song. Introduction to Radio Frequency Interference Prediction and Mission Planning in KARI. *Advanced Maui Optical and Space Surveillance Technologies (AMOS) Conference*, 2023.
[10] P. J. Ryu, S. S. Choi , C. Song, S. Lee , S. Park , D. D-S. Kim. WatcherCatcher: A Real-time Function of SPACEMAP to Predict Spy Satellites in Timeline,*Proceedings of the 73rd International Astronautical Congress*, 18-sep, 2022.